THE ROYAL SOCIETY PUBLISHING

Stochastic modelling of bird flocks: accounting for the cohesiveness of collective motion

Andy M. Reynolds[1], Guillam E. McIvor[2], Alex Thornton[2], Patricia Yang[3,†] and Nicholas T. Ouellette[3]

[1]Rothamsted Research, Harpenden AL5 2JQ, UK
[2]Centre for Ecology and Conservation, University of Exeter, Penryn, Cornwall TR10 9FE, UK
[3]Department of Civil and Environmental Engineering, Stanford University, Stanford, CA 94305, USA

AMR, 0000-0002-7103-3841; AT, 0000-0002-1607-2047

Collective behaviour can be difficult to discern because it is not limited to animal aggregations such as flocks of birds and schools of fish wherein individuals spontaneously move in the same way despite the absence of leadership. Insect swarms are, for example, a form of collective behaviour, albeit one lacking the global order seen in bird flocks and fish schools. Their collective behaviour is evident in their emergent macroscopic properties. These properties are predicted by close relatives of Okubo's 1986 [*Adv. Biophys.* **22**, 1–94. (doi:10.1016/0065-227X(86)90003-1)] stochastic model. Here, we argue that Okubo's stochastic model also encapsulates the cohesiveness mechanism at play in bird flocks, namely the fact that birds within a flock behave on average as if they are trapped in an elastic potential well. That is, each bird effectively behaves as if it is bound to the flock by a force that on average increases linearly as the distance from the flock centre increases. We uncover this key, but until now overlooked, feature of flocking in empirical data. This gives us a means of identifying what makes a given system collective. We show how the model can be extended to account for intrinsic velocity correlations and differentiated social relationships.

1. Introduction

Collective motion attracts intense research interest from physicists, engineers and biologists working on systems from cellular interactions to animal swarms, schools, flocks, herds and human crowds [1,2]. It is therefore rather surprising that we lack a clear, operational definition of what collective behaviour is [3,4]. Typically, we think of collective behaviour as the result of self-organization, whereby simple patterns of interaction between agents lead to the emergence of group-level properties, but these properties are not always clear cut. For instance, bird flocks show collective order with individuals appearing to move together as one [5–11], but swarming midges do not [12]. Similarly, it can be difficult to disentangle truly collective motion from cases where individuals simply happen to be moving independently in the same direction, such as towards a valuable resource. Research has identified several principles that may generate collective motion, such as correlations of individual behaviour [13] and positive feedback loops and nonlinear relationships between individual and group behaviour [14]. However, these principles do not necessarily allow us to specify generic features of collective motion across diverse systems or identify where it occurs.

By drawing an analogy with Newtonian gravitational attraction, Okubo [12] speculated that the interactions between swarming insects produce, on the average, a centrally attractive force that acts on every individual. There is now strong experimental support for such a resultant restoring force in laboratory swarms of *Chironomus riparius* midges [15]. This force increases linearly with increasing distance from the swarm centre, i.e. the insects are behaving on the average as if they are trapped in an elastic potential well and so are analogous to a self-gravitating

system [12,15]. Okubo [12] incorporated this resultant force into a one-dimensional stochastic model. This model and later three-dimensional elaborations [16–21] are in close agreement with a plethora of data from laboratory studies [15,22–25]. Bird flocks may also be analogous to self-gravitating systems as birds may tend to gravitate towards some coarse-grained features of the flock based on the projected view of each individual out through the flock [26]. That is, an individual's visual input is coarse grained to a pattern of [dark] birds against a [light] sky. Visual inputs can also be expected to display fold-change detection which is ubiquitous in nature [27]. Solid angles, like Newtonian gravity, decrease with distance according to an inverse-square power law. Such gravitational-like interactions together with adaptation due to fold-change underpins Okubo's [12] model [16]. This suggests that Okubo's [12] model could be adapted to simulate flocking birds. We show that this is indeed the case, uncovering strong empirical evidence that flocking birds like swarming insects behave on average as if they are trapped in a potential well of their own making. In contrast with laboratory insect swarms, bird flocks possess global order (individual movements are correlated [5]) and interactions between birds can be influenced by social relationships—jackdaws form lifelong monogamous pair-bonds and partners remain in close proximity to one another within flocks in flight [8,28]. Existing models cannot account for this—they assume identical, interchangeable agents. Here following Reynolds [18], we show how velocity correlations and differentiated social relationships can be incorporated into Okubo's [12] model. These new stochastic models are shown to replicate key characteristics of flocks of starlings and jackdaws [8–10,29].

2. Model formulation

Following Okubo [12], we assume that the positions, x_i, and velocities, u_i, of individual birds can be described by the stochastic differential equations

$$\left.\begin{aligned} du_i &= a_i(\mathbf{u},\mathbf{x},t)\,dt + b_{ij}(\mathbf{u},\mathbf{x},t)\,dW_j(t) \\ \text{and} \quad dx_i &= u_i\,dt, \end{aligned}\right\} \quad (2.1)$$

where the subscripts denote individuals (with implied summation over repeated indices) and where $dW(t)$ is an incremental Wiener process with correlation property $\overline{dW_i(t)dW_j(t+t_0)} = \delta(t_0)\delta_{ij}dt$. The function $\mathbf{a}(\mathbf{u},\mathbf{x},t)$ is determined by the requirement that the statistical properties of the simulated positions and velocities be consistent with the observed or assumed form of the joint distribution of velocity and position, $P(\mathbf{u},\mathbf{x},t)$. Mathematically, this requires that $P(\mathbf{u},\mathbf{x},t)$ be a solution of the Fokker–Planck equation

$$\frac{\partial P}{\partial t} + u_i \frac{\partial P}{\partial x_i} = -\frac{\partial}{\partial u_i}(a_i P) + \frac{b^2}{2}\frac{\partial^2 P}{\partial u_i^2}, \quad (2.2)$$

when the magnitude of the driving noise, $\mathbf{b}(\mathbf{u},\mathbf{x},t)$, is taken to be a constant [30]. For statistically stationary flocks having $\partial P/\partial t = 0$,

$$a_i P = \frac{b^2}{2}\frac{\partial P}{\partial u_i} + \phi_i(x,u,t), \quad (2.3)$$

where,

$$\frac{\partial \phi_i}{\partial u_i} = -u_i \frac{\partial P}{\partial x_i}. \quad (2.4)$$

The functional form of $P(\mathbf{u},\mathbf{x},t)$ is not known but the least biased (maximum entropy) form consistent with, spatial location (cohesiveness); alignment; pair-bonding; and a characteristic speed, is a multivariant Gaussian

$$P(\mathbf{u},\mathbf{x},t) = \frac{1}{(2\pi)^N (\mathrm{Det}\lambda\mathrm{Det}\tau)^{1/2}} \exp\left(-\frac{1}{2}(x_i - \bar{x})\right)\tau_{ij}^{-1}(x_j - \bar{x})$$

$$\exp\left(-\frac{1}{2}(u_i - \bar{u})\tau_{ij}^{-1}(u_j - \bar{u})\right), \quad (2.5)$$

where $\bar{x}$ is the centre of mass of the flock, $\bar{u} = d\bar{x}/dt$, $\lambda_{ij} = \langle x_i x_j \rangle$ which is non-zero for paired birds (that tend to remain close together) and zero for unpaired birds and where $\tau_{ij} = \langle u_i u_j \rangle$. A multivariant Gaussian is attained when Shannon's entropy is maximized subject to the constraints imposed by knowing only the first and second moments of the distribution. One of the simplest one-dimensional stochastic models corresponding to equation (2.5) is, from (equations (2.1–2.4)), given by

$$\left.\begin{aligned} du_i &= -\frac{b^2}{2}\tau_{ij}^{-1}(u_j - \bar{u})dt - \tau_{ij}\lambda_{jk}^{-1}(x_k - \bar{x})\,dt \\ &\quad + \frac{1}{2}\frac{\partial\tau_{ij}}{\partial x_j}dt + \frac{1}{2}\tau_{lj}^{-1}\frac{\partial\tau_{il}}{\partial x_k}u_j u_k\,dt + b\,dW_i(t) \end{aligned}\right\} \quad (2.6)$$

$$\text{and} \quad dx_i = u_i\,dt.$$

Details of the derivation of such models can be found in Rodean [31].

— The first term describes how an individual's velocity relaxes to a weighted sum of the velocities of its neighbours.
— The second term describes an individuals' effective attraction to the centre of the flock (due to visual interactions that are not modelled explicitly, see Introduction) and to the other birds in the flock. As argued in the [26] Introduction, such confinement within a harmonic potential is expected if flocking birds interact visually in the way uncovered by Pearce et al. [26]. We do not model these visual interactions explicitly. Instead, their net effort is subsumed into an effective (linear) restoring force term. This is exactly analogous to the case of swarming midges which interact acoustically; these interactions are not modelled explicitly, instead their net effect is subsumed into an effective (linear) restoring force term [12,16,17,19,32]. In both cases, the harmonic potential is an emergent property of the collective behaviours.

It is most readily understood for the case of a flock of non-aligning birds containing a single pair of individuals (individuals 1 and 2) that remain in close proximity, so that

$$\lambda = \sigma_x^2 \begin{bmatrix} 1 & c & 0 \\ c & 1 & 0 \\ 0 & 0 & \ddots \end{bmatrix} \text{ and } \tau = \sigma_u^2 \begin{bmatrix} 1 & 0 & 0 \\ 0 & 1 & 0 \\ 0 & 0 & \ddots \end{bmatrix}.$$

Denoting with A_1 the predicted mean acceleration of bird 1, from (2.6) we get the following expression $A_1 = -\sigma_u^2/\sigma_x^2[1/1 + c(x_1 - \bar{x}) + c/1 - c^2(x_1 - x_2)]$. Bird 1 is therefore attracted to the flock centre and, in accordance with observations [9], also exhibits a spring-like response (rather than an apparent spring-like response due to the pervasiveness of the central attraction, electronic supplementary material) to its partner, with acceleration increasing linearly with distance. As observed [8], this model therefore predicts
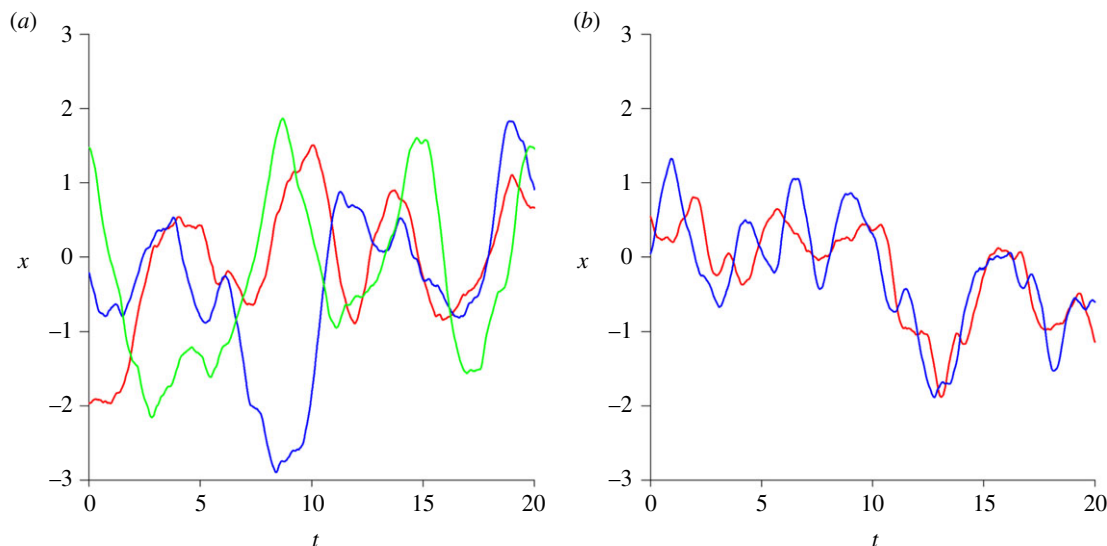
Figure 1. Predicted characteristics of a flock with (a) three unpaired birds and (b) two paired birds. Example trajectories showing that unpaired birds exchange neighbours slowly whereas paired birds maintain an almost fixed distance to the partners. Predictions were obtained using the stochastic model, equation (2.6), with $\bar{x} = 0$ and $\langle x_i x_j \rangle = 0$ for the unpaired and arbitrary units, a.u] for the paired birds. All other model parameters were set to unity [a.u.]. Velocity correlations are absent.

that unpaired birds exchange neighbours slowly whereas paired birds maintain an almost fixed distance to their partners (figure 1). If pervasive, such position-dependent attraction forces can result in milling-like patterns and other kinds of large-scale patterns [33]. Nonetheless, the pairing does not change the net binding of bird 1 to the flock centre, as averaging over x_2 gives $\langle A_1 \rangle = -\sigma_u^2/\sigma_x^2(x_1 - \bar{x})$. Without such central attraction individuals would undergo Richardson-like relative diffusion [34], and consequently simulated flocks would eventually dissolve. Nonetheless, central attraction in bird flocks has not been reported on the literature. It is, however, present in the self-propelled particle model of Ling *et al.* [10] (a modified Viscek [35] model) but only as an *ad hoc* way to confine the flocks without the need for periodic boundary conditions.

Similarly, if $\lambda = \sigma_x^2 \begin{bmatrix} 1 & 0 & 0 \\ 0 & 1 & 0 \\ 0 & 0 & \ddots \end{bmatrix}$ and $\tau = \sigma_u^2 \begin{bmatrix} 1 & c & 0 \\ c & 1 & 0 \\ 0 & 0 & \ddots \end{bmatrix}$ then

$$A_1 = -\frac{\sigma_u^2}{\sigma_x^2}[(1 + c)(x_1 - \bar{x}) - c(x_1 - x_2)].$$

Note also that non-Gaussian density profiles will result in nonlinear effective force terms.

— The third and fourth terms in the stochastic model, equation (2.6), ensure that simulated velocities have the prescribed velocity correlations and are effectively a 'social force' that contributes to velocity changes. These terms ensure that the spatial distribution of individuals is Gaussian on average. Without these terms, individuals would tend to drift apart because relative velocities tend to decrease as individuals come together and increase as they move apart, leading to a net outward drift, a process akin to turbophoresis. The third and fourth terms counter this drift which on average is given by $-\partial \tau_{ij}/\partial x_j$. Turbophoresis could be problematic in other models that incorporate seemingly physically plausible but *ad hoc* interaction terms imposing, for example, alignment of neighbouring birds or repulsion between closely neighbouring birds. In this regard, it is worth noting that the

third term induces short-range 'repulsive' interactions when velocity correlations are positive [36]. The third and fourth terms vanish when birds interact with a fixed number of neighbours, rather than with all neighbours with a fixed metric distance. Such topological interactions (nth nearest neighbour interactions irrespective of their distance) arise in jackdaw flocks when travelling to roosts and in starling murmurations [5,10,37]. Metric (scale finite) interactions are evident in jackdaw flocks during anti-predator mobbing events [10]. Because of the functional form of the third and fourth terms, velocity correlations strengthen the long-range central attraction, as first noted by Reynolds [18] (figure 2a). However, when a pair of simulated birds are much closer than the correlation length scale the acceleration between them becomes strongly repelling (figure 2b). Short-range repulsion is therefore a model prediction rather than a model ingredient. Moreover, in accordance with observations [8], pairing causes variations in the local interactions (figure 2b). As observed, for paired birds, the long-range attraction is much stronger, and the repulsion is shorter ranged.

— The fifth term in the stochastic model, equation (2.6), the noise term, represents fluctuations in the resultant internal force that arise partly because of the limited number of individuals in the grouping and partly because of the non-uniformity in their spatial distribution.

When the second (attraction) term vanishes, the three-dimensional form of equation (2.6) is identical to the stochastic model of Sawford *et al.* [38] for the dispersal of multiple tracer particles in high Reynolds number turbulence—a model that provides a good representation of shape statistics for clusters of particles. When spatial and velocity correlations are absent, i.e. when $\lambda_{ij} = \sigma_x^2 \delta_{ij}$ and $\tau_{ij} = \sigma_u^2 \delta_{ij}$, equation (2.6) reduces to Okubo's [12] model for the trajectories of swarming insects

$$\left.\begin{aligned} du_i &= -\frac{b^2}{2}u_i \, dt - \frac{\sigma_u^2}{\sigma_x^2}x_i \, dt + b\,dW_i(t) \\ \text{and} \qquad dx_i &= u_i \, dt, \end{aligned}\right\} \quad (2.7)$$
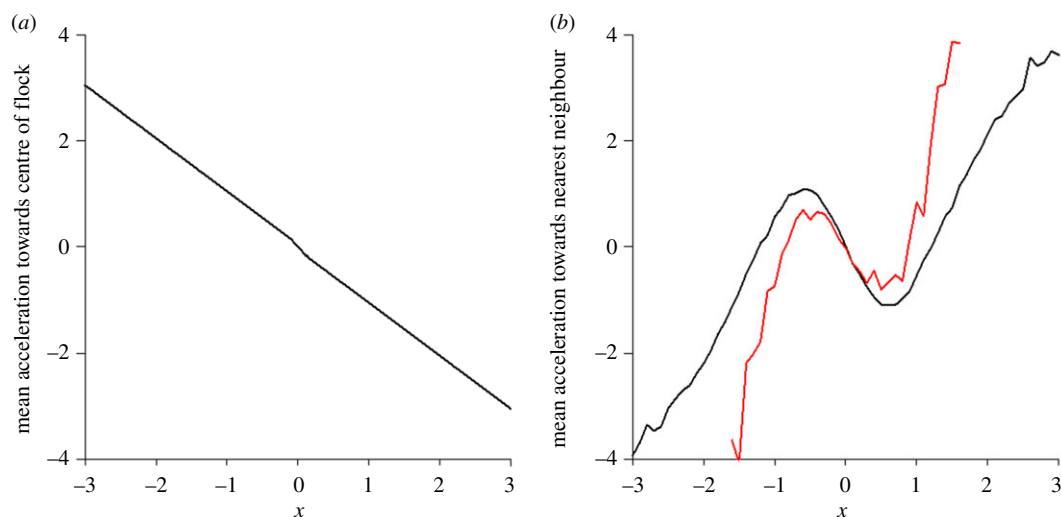
Figure 2. Predicted influence of velocity correlations. (*a*) In the core of the flock, $|x| < 1/2$, the central attraction is strengthened (albeit only slightly as evidenced by the slight kink). (*b*) Correlations induce short-range repulsive interactions and long-range attractive interactions between nearest neighbours, i.e. neighbouring individuals accelerate away from one another when close together and accelerate towards one another when far apart (black line). They also induce long-range attractive interactions between more distant neighbours (data not shown). In accordance with observations [8], pairing causes variations in the local interactions. For paired birds, the long-range attraction is much stronger, and repulsion is shorter ranged (red line). Predictions for flocks without discrete pairs were obtained using the stochastic model, equation (2.6), with $\bar{x} = 0$, $N = 10$ and with all other model parameters set to unity [a.u.]. Paired birds have $\langle x_i x_j \rangle = 0.9$. Velocity correlations were taken to decrease exponentially with separation according to $\tau_{ij} = \sigma_u^2 \exp\left(-(x_i - x_j)^2/2\sigma_c^2\right)$ where σ_c is the correlation length scale and so are scale finite as observed in jackdaw flocks during anti-predator mobbing events [10].

For the sake of clarity, we report on the results of simulations using one-dimensional models, (equation (2.6)), reporting on more complicated higher dimensional models in the electronic supplementary material. Moreover, because we are making qualitative rather than quantitative comparisons with observations all model parameter values are set to unity unless stated otherwise.

3. Flocking birds are trapped in potential wells

The stochastic modelling rests on the assumption that, like insects within a swarm, birds within a flock behave on average as if they are trapped in an elastic potential well. That is, each bird effectively behaves as if it is bound to the flock by a force that on average increases linearly as the distance from the flock centre increases. Here, we provide empirical evidence for this key predicted characteristic of flocking birds which until now has escaped attention. We analysed previously collected datasets of flocking jackdaws (*Corvus monedula*) in two distinct ecological contexts: transit flights from daytime foraging sites to night-time roosts and mobbing of a model terrestrial predator. In both cases, we used ground-based camera arrays to record the three-dimensional, time-resolved flight trajectories of each individual bird in the flocks. Details of our tracking methods can be found in Ling *et al.* [39]. The transit flock datasets are described in Ling *et al.* [8] and the mobbing flock datasets in Ling *et al.* [10].

For both transit and mobbing flocks, we computed mean accelerations as a function of distance from the instantaneous centre of mass of the flock (for transit flocks) and from the time-averaged centre of mass (for mobbing flocks); we note that computing a time-averaged centre of mass for transit flocks is not possible since they systematically move in a directed fashion. In accordance with theoretical expectations, we find that to good approximation mean accelerations conditioned on position increase linearly with the distance from

the centre of the flock, i.e. the birds behave on average as if they are trapped in a potential well of their own making (figure 3). Even though the interactions are different in transit and mobbing flocks [10], both types of flocks display this emergent potential well. We also find that this potential well is largely independent of the flock size. We thereby conjecture that emergent potential wells are a signature feature of collective—a conjecture that is supported by their identification in insect swarms [12,15,40].

4. Comparisons with published observations

4.1. Reshuffling of individuals

The network of interactions within a flock changes over time. Two birds that become strongly correlated because they are nearest neighbours may later become distant neighbours. This dynamic may reinforce correlations between individuals, strongly enhancing global ordering [41]. Group membership may lower an individual's risk of predation. But not all positions within a flock are equivalent, as birds on the boundaries of the flock may be more at-risk [42]. If this cost–benefit trade-off were unfavourable for too many birds, then the flock would break up. Flock stability is therefore contingent on network dynamics that allow for the systematic redistribution of risk among individuals [43]. Cavagna *et al.* [6] reported that at intermediate times birds move faster than Brownian motion with respect to both the centre of mass, and with respect to each other. Reshuffling with these characteristics is predicted in the stochastic models. The stochastic model (equation (2.6)) necessarily predicts that individual movements with respect to the centre of mass and with respect to each other are ballistic at short times (less than the velocity autocorrelation timescale) and diffusive at long time (albeit with vanishing diffusivity because the flocks are localized around their centres of mass) [34].
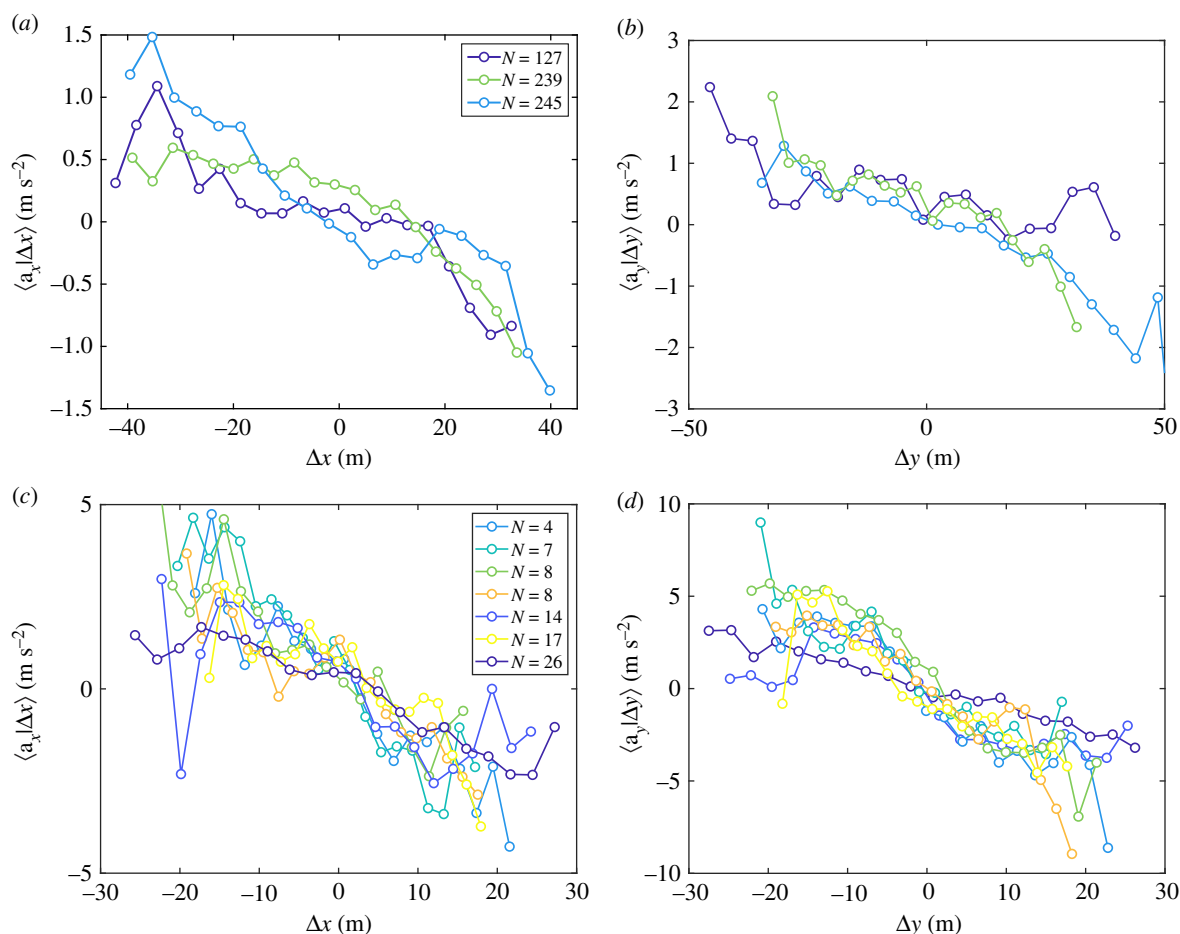
Figure 3. Empirical evidence for central forces in jackdaw flocks. Mean acceleration components are computed as a function of distance from the flock centre of mass for (*a*,*b*) transit flocks and (*c*,*d*) mobbing flocks (see text for the distinction). For transit flocks, the centre of mass is computed instantaneously at each time step; for mobbing flocks, it is averaged over time. The *x* direction is taken to be the instantaneous travel direction of the flock, and the *y* direction is the transverse direction, orthogonal to both *x* and the gravity direction. Each colour shows data for a different flocking event. The three transit flocks analysed contained 127, 245 and 239 individuals, and the seven mobbing flocks contained 4, 7, 8, 8, 14, 17 and 26 individuals. In all cases, the conditional mean accelerations are linear in the distance to the flock centre with a negative slope, indicating a harmonic potential field. The root-mean-square error of linear fits to the data between −20 m and 20 m is 0.11 m s^{-2} for (*a*) (averaged over all three curves) and 0.15 m s^{-2} for (*b*). Similar fits to the data between −10 m and 10 m give average root-mean-square errors of 0.46 m s^{-2} for (*c*) and 0.58 m s^{-2} for (*d*).

4.2. Transport of information in turning flocks

Attanasi *et al.* [29] (see also Procaccini *et al.* [44]) identified nearly lossless propagation through the flock of turns made by individual starlings; a phenomenon that was modelled by [45] and by Cristiani *et al.* [46]. Nearly lossless propagation is also evident in the global turning behaviours of our simulated flocks. Following the methods of analysis of [29], we examine how turning (as exemplified in figure 4*a*) propagates through a simulated flock. To do this, we first rank all the birds in flocks according to their turning order. Each bird, *i*, is then labelled according to its rank, r_i, and by, the time t_i, at which it began turning. Plots of r_i as a function of t_i reveal that, as with starlings [29], turning of the simulated flock starts with very few birds (figure 4*b*). To understand how turns propagate through the flock, Attanasi *et al.* [29] calculated the radius of the sphere containing all birds that had turned as a function of time. As with starlings [29] and jackdaws [9], this radius increases linearly with time at early times (figure 4*c*) and turns propagate across the flock with negligible attenuation thereby keeping group decoherence to a minimum (figure 4*a*). In accordance with observations [9],

the speed of propagation, c_s, increases with flock size for small flocks, but saturates for larger groups (figure 4*d*).

4.3. Transition from disordered aggregations to order motion as the group density increases

Ling *et al.* [10] reported that jackdaws interact with a fixed number of neighbours (topological interactions) when travelling to roosts but coordinate with neighbours based on spatial distance (metric interactions) during anti-predator 'mobbing' events. Consequently, mobbing flocks exhibit a transition from disordered aggregations to ordered motion as the group density increases. At low density, flocks resemble disordered swarms (as predicted because the stochastic model reduces to Okubo's [12] stochastic model for insect swarms). At moderate density, flocks show some degree of coherence, and at high density, all the jackdaws move and turn as a coherent unit [10]. Ling *et al.* [10] quantified coherence with the order parameter $\phi = |\langle u_i / |u_i| \rangle|$ where $\langle \rangle$ denotes an average over all birds. The observed relationship between group density and group order during this transition agrees well with the stochastic model (figure 5).
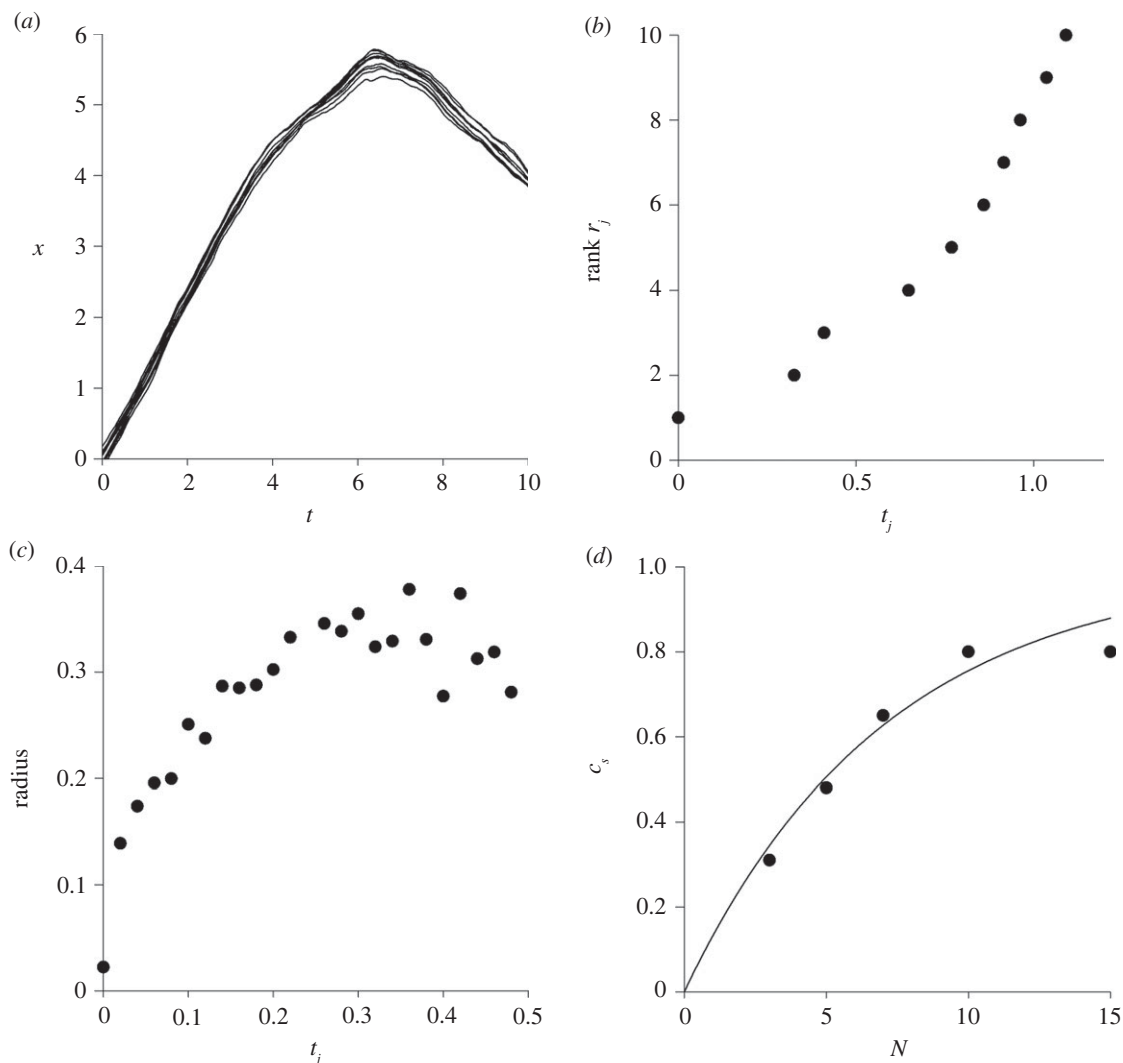
Figure 4. Predicted propagation of a turn across a correlated flock. (a) Example trajectories showing cohesion and a collective turn. Accelerations decrease only weakly in passing from the first to the last turning birds in the flock. (b) The order of each bird in the turning sequence as a function of the turning time. At early times, few birds turn. (c) The radius of the sphere containing all birds that have turned. (d) The speed of propagation, c_s (closed black circle) and the empirical fit to observations, $c_s = 1 - e^{-N/7.1}$ [9]. Linear regression of our predictions for $ln(1 - c_s)$ on N/N_o gives a best fit exponential decay rate $N_o = 7.7$ individuals. Observations fall within the 95% confidence intervals of 6.7 and 9.09 individuals. At short times, the radius increases linearly with time: $r = c_s t$. Predictions were obtained using the stochastic model, equation (2.6), with, $N = 10$, $\langle x_i x_j \rangle = 0$ and $\sigma_x = 0.1$ and all parameters set to unity [a.u.] (a–c). At time $t = 0^-$, all individuals are moving with the same velocity (1,0). Speeds were estimated by linear regression of the radius on time t_j, for $0 < t_j < 0.3$. Velocity correlations were taken to decrease exponentially with separation according to $\tau_{ij} = \sigma_u^2 \exp\left(-(x_i - x_j)^2/2\sigma_c^2\right)$ where σ_c is the correlation length scale and so are scale finite as observed in jackdaw flocks during anti-predator mobbing events [10].

This relationship is also predicted by the self-propelled particle model of Ling *et al.* [10] which like the stochastic model, equation (2.6), incorporates a centrally attractive 'gravitational-like' force that acts on every individual. As expected, and observed, order in transit flocks is predicted to be independent of density (figure 5).

5. High-density outer borders and distinguishable subgroups

Flocks of starlings tend to have high-density outer borders and flocks of jackdaws in transit can consist of several distinguishable subgroups separated along the movement direction [11,37]. These phenomena may be related and could be incorporated into the modelling framework if individuals are attracted to the centres of local clusters rather than to the global centre of mass—as might be expected in self-gravitating systems. Here, this was done by continually partitioning flocks

into subgroups using *k*-means clustering. Simulated flocks typically fragment into spatially distinct subgroups, i.e. into flocks with high-density outer borders (figure 6). Previous stochastic models have either neglected to account for the high-density borders [41] or have effectively used the observed form as a model input [47]. Although accidental, the high-density borders may be biologically significant, creating a 'wall effect' that confuses predators [37]. To date, no other putative mechanism for producing high-density borders have been identified, although Cavagna *et al.* [6] did suggest that flocks may self-organize out of the selfish tendency of individuals not to stay at the border, a situation reminiscent of Hamilton's [48] 'selfish herd' scenario (but see [49]).

6. Discussion

Bird flocks and insect swarms are two seemingly starkly different forms of collective behaviour that serve to highlight
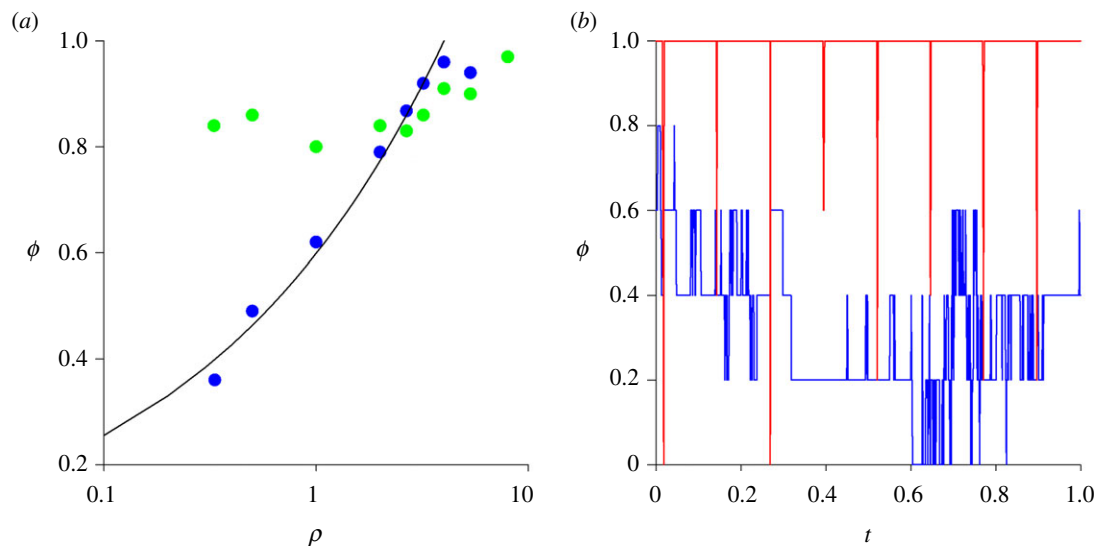
Figure 5. Predicted relationship between group density and group order. (a) In accordance with observations, polarization in mobbing flocks with metric correlations (closed blue circle), ϕ, increases monotonically with density, ρ, following a power law $\phi \sim \rho^{0.37}$ (solid line) before saturating [10]. For flocks with topological (scale-free) interactions, order is observed and predicted to be independent of density (closed green circle) [10]. Predictions (closed black circle) for mobbing flocks were obtained using the stochastic model, equation (2.6), with $\bar{x} = 0$, $\langle x_i x_j \rangle = 0$, $N = 10$ and with σ_x ranging between 1/8 and 3 [a.u.]. Velocity correlations were taken to decrease exponentially with separation according to $\tau_{ij} = \sigma_u^2 \exp\left(-(x_i - x_j)^2 / 2\sigma_c^2\right)$ where σ_c is the correlation length scale and so are scale finite as observed in jackdaw flocks during anti-predator mobbing events [10]. All other model parameters were set to unity [a.u.]. Predictions for the scale-free flocks were obtained for $\tau_{ij} = \sigma_u^2$ when $i = j$ and $\tau_{ij} = 0.95\sigma_u^2$ for $i \neq j$. (b) Predicted instantaneous polarizations for high ($\sigma_x = 1/8$) (red line) and low ($\sigma_x = 1$) (blue line) density flocks.
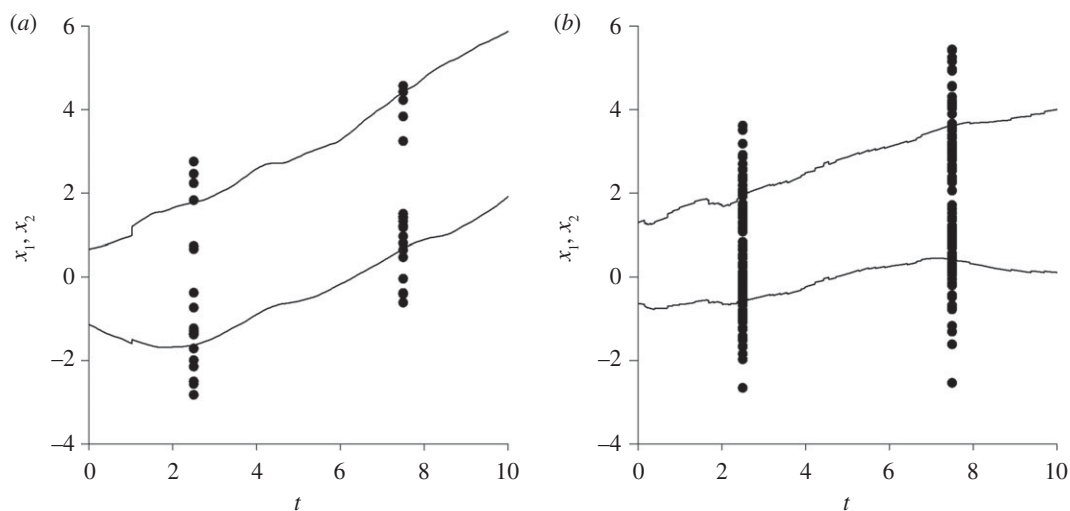

Figure 6. Predicted emergence of high-density borders (distinguishable subgroups separated in space). Predictions were obtained using the stochastic model, equation (2.6), for a flock with (a) $N = 20$ and (b) $N = 100$ birds interacting topologically ($\tau_{ij} = 0.5$). All other parameters were set to unity [a.u.]. The flock was continuously partitioned into two subgroups with centres x_1 and x_2 using the standard 'naive' k-means algorithm. Snap shots of positional fixes of individual birds are shown (closed black circle). More examples are presented in the electronic supplementary material.

the difficulties faced when attempting to define collective movements in a way that can be operationalized across systems. Here, we argued that Okubo's [12] model of insect swarms encapsulates the cohesiveness mechanism at play in bird flocks. We showed for the first time that flocking birds do indeed behave on average as if they are trapped in an elastic potential well, just as predicted (figure 3). We therefore suggest that emergent potential wells are a signature feature of collective movements and a plausible way to distinguish a group that is not collective from one that is, in that the members of a collective group feel an attraction to each other. These potential wells bind flocks together and are significant because cohesion rather than coherent

motion is the most basic property of collective movements. We then showed how the distinctive features of bird flocks, intrinsic velocity correlations (global ordering) [5,37,43] and differentiated social relationships [8–11] that are not present in insect swarms [50] can be incorporated into Okubo's [12] model (figure 1). The simplest such model, a minimally structured (maximum entropy) model, predicts that discrete pairs of individuals are tied together by spring-like effective forces, as evidenced in jackdaws, a species that forms lifelong pair-bonds [8] (figure 2). This model was also found to describe the salient features of collective turns, principally nearly loss-less propagation of turning behaviour and linear-in-time growth of the transfer of information distance [9,29]

(figure 4). And it predicts correctly how mobbing flocks of jackdaws transition from disordered aggregations to ordered motion as the group density increases [10] (figure 5). It was shown how the modelling approach can be extended to account for the presence of high-density outer borders and subgroups [11,37] (figure 6). Previous models [26,41,45–47] capture some but not all these facets of flocking. Any future models that account for the observations will have more structure than our minimally structured model and hence (explicitly or implicitly) will assume something more about the flock beyond what is required to match the data.

Variants of Okubo's [12] model therefore predict correctly the markedly different properties of bird flocks and insect swarms. Swarms do, for example, strongly damp perturbations [20]. Thus, unlike bird flocks, which appear to use collective behaviour to promote lossless propagation of information flow through flocks [29], swarms use it to stabilize themselves against environmental perturbation. In the modelling, this distinction can be attributed to the simulated flocks being freely roaming whereas the swarms are localized. Other differences between the predicted behaviours of swarms and flocks can be attributed to the presence/absence of correlations and perhaps also to dimensionality: swarms are three-dimensional [15], flocks are one- or two-dimensional [43].

The modelling also predicts that Newton's third law is violated when the interactions are metric because the effective spring constants are velocity dependent. This is not problematic because Newton's third law need not be respected in biological aggregates [4,33]. More generally,

violations of Newton's third law, in the form of velocity-dependent effective spring constants, become unavoidable when the velocity statistics are assumed to be non-Gaussian rather than Gaussian, as would be the case if a threshold is put on the maximum possible flight speed [16].

The formulation of stochastic models for two- and three-dimensional flocks with central attraction and correlations is challenging and is outlined in the electronic supplementary material. A more substantial challenge is the formulation of stochastic models that satisfy the so-called 'two-to-one' reduction. The statistics of flocks containing $N-1$ birds calculated from stochastic models of flocks containing $N-1$, N, $N+1,\ldots$ birds are not equivalent [34,51].

References

1. Couzin ID. 2018 Synchronization: the key to effective communication in animal collectives. *Trends. Cog. Sci.* **22**, 844–846. (doi:10.1016/j.tics.2018.08.001)

2. Ouellette NT, Gordon DM. 2021 Goals and limitations of modeling collective behavior in biological systems. *Front. Phys.* **9**, 687823. (doi:10.3389/fphy.2021.687823)

3. Ouellette NT. 2017 Toward a 'thermodynamics' of collective behavior. *SIAM News* **50**.

4. Ouellette NT. 2019 The most active matter of all. *Matter* **1**, 297–299. (doi:10.1016/j.matt.2019.07.012)

5. Cavagna A, Cimarelli A, Giardina I, Parisi G, Santagati R, Stefanini F, Viale M. 2010 Scale-free correlations in starling flocks. *Proc. Natl Acad. Sci. USA* **107**, 11 865–11 870. (doi:10.1073/pnas.1005766107)

6. Cavagna A, Queiros SMD, Giardina I, Stefanini F, Viale M. 2013 Diffusion of individual birds in starling flocks. *Proc. R. Soc. B* **280**, 20122484. (doi:10.1098/rspb.2012.2484)

7. Cavagna A, Giardina I, Grigera TS, Jelic A, Levine D, Ramaswamy S, Viale M. 2015 Silent flocks: constraints on signal propagation across biological groups. *Phys. Rev. Lett.* **114**, 218101. (doi:10.1103/PhysRevLett.114.218101)

8. Ling H, McIvor GE, Van Der Vaart K, Vaughan RT, Thornton A, Ouellette NT. 2019 Costs and benefits of social relationships in the collective motion of

bird flocks. *Nat. Ecol. Evol.* **3**, 943–948. (doi:10.1038/s41559-019-0891-5)

9. Ling H, McIvor GE, Westley J, Van Der Vaart K, Yin J, Vaughan RT, Thornton A, Ouellette NT. 2019 Collective turns in jackdaw flocks: kinematics and information transfer. *J. R. Soc. Inter.* **16**, 20190450. (doi:10.1098/rsif.2019.0450)

10. Ling H, McIvor GE, Westley J, Van Der Vaart K, Vaughan RT, Thornton A, Ouellette NT. 2019 Behavioural plasticity and the transition to order in jackdaw flocks. *Nat. Comm.* **10**, 5174. (doi:10.1038/s41467-019-13281-4)

11. Ling H, McIvor GE, Van Der Vaart K, Vaughan RT, Thornton A, Ouellette NT. 2019 Local interactions and their group-level consequences in flocking jackdaw. *Proc. R. Soc. B* **286**, 20190865. (doi:10.1098/rspb.2019.0865)

12. Okubo A. 1986 Dynamical aspects of animal grouping: swarms, schools, flocks and herds. *Adv. Biophys.* **22**, 1–94. (doi:10.1016/0065-227X(86)90003-1)

13. Attanasi A *et al.* 2014 Collective behaviour without collective order in wild swarms of midges. *PLoS Comp. Biol.* **10**, e1003697. (doi:10.1371/journal.pcbi.1003697)

14. Sumpter DJ. 2006 The principles of collective animal behaviour. *Phil. Trans. R. Soc. B* **361**, 5–22. (doi:10.1098/rstb.2005.1733)

15. Kelley DH, Ouellette NT. 2013 Emergent dynamics of laboratory insect swarms. *Sci. Rep.* **3**, 1–7. (doi:10.1038/srep01073)

16. Reynolds AM, Sinhuber M, Ouellette NT. 2017 Are midge swarms bound together by an effective velocity-dependent gravity? *Euro. Phys. J. E* **40**, 46. (doi:10.1140/epje/i2017-11531-7)

17. Reynolds AM. 2018 Langevin dynamics encapsulate the microscopic and emergent macroscopic properties of midge swarms. *J. R. Soc. Inter.* **15**, 20170806. (doi:10.1098/rsif.2017.0806)

18. Reynolds AM. 2019 On the origin of the tensile strength of insect swarms. *Phys. Biol.* **16**, 046002. (doi:10.1088/1478-3975/ab12b9)

19. Reynolds AM. 2019 On the emergence of gravitational-like forces in insect swarms. *J. R. Soc. Inter.* **16**, 20190404. (doi:10.1098/rsif.2019.0404)

20. van der Vaart, Sinhuber M, Reynolds AM, Ouellette NT. 2019 Mechanical spectroscopy of insect swarms. *Sci. Adv.* **5**, eaaw9305. (doi:10.1126/sciadv.aaw9305)

21. van der Vaart, Sinhuber M, Reynolds AM, Ouellette NT. 2020 Environmental perturbations induce correlations in midge swarms. *J. R. Soc. Inter.* **17**, 20200018. (doi:10.1098/rsif.2020.0018)

22. Ni R, Puckett JG, Dufresne ER, Ouellette NT. 2015 Intrinsic fluctuations and driven response of insect swarms. *Phys. Rev. Lett.* **115**, 118104. (doi:10.1103/PhysRevLett.115.118104)

23. Ni R, Ouellette NT. 2016 On the tensile strength of insect swarms. *Phys. Biol.* **13**, 045002. (doi:10.1088/1478-3975/13/4/045002)

24. Sinhuber M, Ouellette NT. 2017 Phase coexistence in insect swarms. *Phys. Rev. Lett.* **119**, 178003. (doi:10.1103/PhysRevLett.119.178003)

25. Sinhuber M, Van Der Vaart K, Ouellette NT. 2019 Response of insect swarms to dynamic illumination perturbations. *J. R. Soc. Inter.* **16**, 20180739. (doi:10.1098/rsif.2018.0739)

26. Pearce DJG, Miller AM, Rowlands G, Turner MS. 2014 Role of projection in the control of bird flocks. *Proc. Natl Acad. Sci. USA* **111**, 10 422–10 426. (doi:10.1073/pnas.1402202111)

27. Shoval O, Goentoro L, Hart Y, Mayo A, Sontag E, Alon U. 2010 Fold-change detection and scalar symmetry of sensory input fields. *Proc. Natl Acad. Sci. USA* **107**, 15 995–16 000. (doi:10.1073/pnas.1002352107)

28. Jolles JW, King AJ, Manica A, Thornton A. 2013 Heterogeneous structure in mixed-species corvid flocks in flight. *Anim. Behav.* **85**, 743–750. (doi:10.1016/j.anbehav.2013.01.015)

29. Attanasi A *et al.* 2014 Information transfer and behavioural inertia in starling flocks. *Nat. Phys.* **10**, 691–696. (doi:10.1038/nphys3035)

30. Thomson DJ. 1987 Criteria for the selection of stochastic models of particle trajectories in turbulent flows. *J. Fluid Mech.* **180**, 529–556. (doi:10.1017/S0022112087001940)

31. Rodean HC. 1996 Stochastic Lagrangian models of turbulent diffusion. *Meteorol. Monographs,* **26**, 1 –84.

32. Reynolds AM, Ouellette NT. 2016 Swarm dynamics may give rise to Lévy flights. *Sci. Rep.* **6**, 30515. (doi:10.1038/srep30515)

33. Barberis L, Peruani F. 2016 Large-scale patterns in a minimal cognitive flocking model: incidental leaders, nematic patterns, and aggregates. *Phys. Rev. Lett.* **117**, 248001. (doi:10.1103/PhysRevLett.117.248001)

34. Thomson DJ. 1990 A stochastic model for the motion of particle pairs in isotropic high-Reynolds-number turbulence, and its application to the problem of concentration variance. *J. Fluid Mech.* **210**, 113–153. (doi:10.1017/S0022112090001239)

35. Viscek T, Czirok A, Ben-Jacob E, Cohen I, Shochet O. 1995 Novel type of phase transition in a system of self-driven particles. *Phys. Rev. Lett.* **75**, 1226–1229. (doi:10.1103/PhysRevLett.75.1226)

36. Passino KM. 2013 Modelling and cohesiveness analysis of midge swarms. *Int. J. Swarm Int. Res.* **4**, 1–22. (doi:10.4018/ijsir.2013100101)

37. Ballerini M *et al.* 2008 Interaction ruling animal collective behaviour depends on topological rather than metric distance: evidence from a field study. *Proc. Natl Acad. Sci. USA* **105**, 1232–1237. (doi:10.1073/pnas.0711437105)

38. Sawford BL, Pope SB, Yeung PK. 2013 Gaussian Lagrangian stochastic models for multi-particle dispersion. *Phys. Fluid* **25**, 055101. (doi:10.1063/1.4802037)

39. Ling H, McIvor GE, Nagy G, MohaimenianPour S, Vaughan RT, Thornton A, Ouellette NT. 2018 Simultaneous measurements of three-dimensional trajectories and wingbeat frequencies of birds in the field. *J. R. Soc. Inter.* **15**, 20180653. (doi:10.1098/rsif.2018.0653)

40. Woodgate JL *et al.* 2021 Harmonic radar tracking reveals that honeybee drones navigate between multiple aerial leks. *Iscience* **24**, 102499. (doi:10.1016/j.isci.2021.102499)

41. Bialek W, Cavagna A, Giardina I, Mora T, Silvestri E, Viale M, Walczak AM. 2012 Statistical mechanics for natural flocks of birds. *Proc. Natl Acad. Sci. USA* **109**, 4786–4791. (doi:10.1073/pnas.1118633109)

42. Lambert PJ, Herbert-Read JE, Ioannou CC. 2021 The measure of spatial position within groups that best predicts predation risk depends on group movement. *R. Soc. Proc. B* **288**, 20211286. (doi:10.1098/rspb.2021.1286)

43. Ballerini M *et al.* 2008 Empirical investigation of starling flocks: a benchmark study in collective animal behaviour. *Anim. Behav.* **76**, 201–215. (doi:10.1016/j.anbehav.2008.02.004)

44. Procaccini A *et al.* 2011 Propagating waves in starling, *Sturnus vulgaris*, flocks under predation. *Anim. Behav.* **82**, 759–765. (doi:10.1016/j.anbehav.2011.07.006)

45. Cavagna A *et al.* 2015 Flocking and turning: a new model for self-organized collective motion. *J. Stat. Phys.* **158**, 601–627. (doi:10.1007/s10955-014-1119-3)

46. Cristiani E, Menci M, Papi M, Brafman L. 2021 An all-leader agent-based model for turning and flocking birds. *J. Math. Biol.* **83**, 1–22. (doi:10.1007/s00285-021-01675-2)

47. Lewis JM, Turner MS. 2017 Density distributions and depth in flocks. *Phys. D* **50**, 494003. (doi:10.1088/1361-6463/aa942f)

48. Hamilton WD. 1971 Geometry for the selfish herd. *J. Theor. Biol.* **31**, 295–311. (doi:10.1016/0022-5193(71)90189-5)

49. Sankey DW, Storms RF, Musters RJ, Russell TW, Hemelrijk CK, Portugal SJ. 2021 Absence of 'selfish herd' dynamics in bird flocks under threat. *Curr. Biol.* **31**, 3192–3198. (doi:10.1016/j.cub.2021.05.009)

50. Ni R, Ouellette NT. 2015 Velocity correlations in laboratory insect swarms. *Eur. Phys. J. Spec. Top.* **224**, 3271–3277. (doi:10.1140/epjst/e2015-50077-5)

51. Borgas MS, Sawford BL. 1994 A family of stochastic models for two-particle dispersion in isotropic homogeneous stationary turbulence. *J. Fluid Mech.* **279**, 69–99. (doi:10.1017/S0022112094003824)

52. Gorbonos D, Ianconescu R, Puckett JG, Ni R, Ouellette NT, Gov NS. 2016 Long-range acoustic interactions in insect swarms: an adaptive gravity model. *New J. Phys.* **18**, 073042. (doi:10.1088/1367-2630/18/7/073042)

53. Gorbonos D, Gov NS. 2017 Stable swarming using adaptive long-range interactions. *Phys. Rev. E* **95**, 042405. (doi:10.1103/PhysRevE.95.042405)

54. Puckett JG, Kelley DH, Ouellette NT. 2014 Searching for effective forces in laboratory insect swarms. *Sci. Rep.* **4**, 4766. (doi:10.1038/srep04766)

55. Reynolds AM. 2018 Fluctuating environments drive insect swarms into a new state that is robust to perturbations. *Europhys. Lett.* **124**, 38001. (doi:10.1209/0295-5075/124/38001)

56. Sinhuber M, Van Der Vaart K, Feng Y, Reynolds AM, Ouellette NT. 2021 An equation of state for insect swarms. *Sci. Rep.* **11**, 3773. (doi:10.1038/s41598-021-83303-z)

57. Storms RF, Carere C, Zoratto F, Hemelrijk CK. 2019 Complex patterns of collective escape in starling flocks under predation. *Behav. Ecol. Sociobiol.* **73**. (doi:10.1007/s00265-018-2609-0)

58. Usherwood JR. 2011 Flying in a flock comes at a cost in pigeons. *Nature* **474**, 494–497. (doi:10.1038/nature10164)